We are IntechOpen, the world's leading publisher of Open Access books Built by scientists, for scientists

4,800
Open access books available

122,000
International authors and editors

135M
Downloads

Our authors are among the

154
Countries delivered to

TOP 1%
most cited scientists

12.2%
Contributors from top 500 universities

WEB OF SCIENCE™

Selection of our books indexed in the Book Citation Index in Web of Science™ Core Collection (BKCI)

Interested in publishing with us?
Contact book.department@intechopen.com

Numbers displayed above are based on latest data collected.
For more information visit www.intechopen.com

12

Hydrodynamic Influences on Fluid Mud Distribution in the Amazon Subaqueous Delta

Roberto Fioravanti Carelli Fontes[1], Áurea Maria Ciotti[2] and Belmiro Mendes de Castro[3]
[1]*Universidade Estadual Paulista (Campus do Litoral Paulista)*
[2]*Universidade de São Paulo (Centro de Biologia Marinha)*
[3]*Universidade de São Paulo (Instituto Oceanográfico)*
Brazil

1. Introduction

Transport and distribution of sediments in the Amazon Subaqueous Delta and the Amazon Shelf (ASD; AS) depend upon of the loads in the Amazon River Basin and on the hydrodynamics aspects. The latter, on the other hand, reacts to the distribution of sediment patches due to decreasing of the bottom stress parameter on finer sediments and fluid mud regions, mostly located on the inner shelf. The Amazon River discharge, tides and stratification are the dominant forcing for currents and related phenomena on the inner AS.
In order to study the physical aspects related to sediment transport in the ASD, we applied the Estuarine and Coastal Ocean Model and Sediment Transport (ECOMSED). This model is capable of simulating both hydrodynamics and sediment dynamics processes in coastal regions. In this chapter, we present results from hydrodynamic modeling experiments, taking into account the complexity of the AS dynamics, including the river plume fate and shape, as well as the frontal zone positioning. The North Brazil Current and other oceanic processes have not been considered in this study, since their main influences occur in the outer shelf, far beyond the river mouth.
The Amazon River Estuary (ARE) does not fit into a classical definition of an estuary, once the mixing zone is not constrained by its margins, appearing in the open shelf. The haline front develops further ahead from the river mouth, preserving most of its characteristics, without being in an estuarine channel. The ASD consists of reworked sediment deposits located seward of the river mouth, on the inner continental shelf. Kineke et al. (1996) defined as fluid mud, the extensive regions of dense nearbed suspensions of sediments where concentrations are above 10 g L^{-1} . Thickly patches of fluid mud layers affect circulation by decreasing the bottom stress coefficient and enhancing tidal currents and the sea level oscillations. Model calibration considered a variable bottom stress distributed according to the ASD, accommodating the reworked sediments and fluid mud parameterizations. Values for these parameters ranged from 2.0 10^{-5}, in fluid mud regions, to 3.2 10^{-3}, in the reworked sediments background. The patches of fluid mud and reworked sediments define, on their vicinities, regions of strong bottom stress gradients capable of promoting residual vorticity and residual circulation.
Residual flows in marine environments can be generated by wind stress variability, by horizontal density gradients, by barotropic effects due to remote processes or by nonlinear tide

current interactions, when energy cascades from dominant frequencies to its harmonics. Tidal currents flowing over coastal areas, subjected to irregular bathymetry, produces residual flow due to nonlinear interactions. Results from numerical experiments focused on the generation of residual vorticity, due to nonlinear interactions and anisotropy of sediment distribution, suggest that residual flow may be enhanced on the ASD region. We evaluated and discussed the role and magnitude of various terms related to residual vorticity as tendency; advection; roughness; dissipation; velocity; bathymetry and Coriolis. The roughness term is the most relevant on vicinity of transitional regions of distinguished sediment patches. Although residual currents are about one order of magnitude lesser than tidal currents, they can be relevant in long-term component of suspended sediment transport and transport of living matter, as algae and larvae in the AS.
The Amazon River Plume (ARP) defines the front position on the continental shelf, as well as the region of maximum sediment deposition rates, or maximum turbidity zone. According to the hydraulic control theory, we could define an internal, or composite Froud Number, which aims to describe the region where hydraulic control occurs. Seaward of this control region a hydraulic jump defines the location where the ARP disconnects from the bottom and acquires negative vorticity, by turning southeastward. Afterwards, the trade winds and the North Brazil Current drive the ARP northwestward, along the coast of Amapá.
Finally, we discuss the leading mechanisms on generation and maintenance of the salinity and turbidity fronts, which are the keys on fluid mud layer formation. Tides promote vertical shear homogenization due to interactions of currents with topography, via hydraulic control, acting as a maintainer of the haline front position and defining the maximum turbidity zone in the ASD.

1.1 Outline & rationale

Some charactericstics of the AS are described in Section 2, related to the hydrodynamics and morphology of the ASD and its environmental description. The numerical model ECOMSED and data are desccribed in Section 3, considering the hydrodynamic core of the model and its sediment transport module. In Section 3.2 there is a detailed consideration on influences of sediment patches (including the fluid mud layer), and parameterization of the bottom stress, a crutial step on modeling the dynamics of currents and tides in coastal environments.
The ARE is an unique estuarine environment, mostly related to the positioning of its salinity front at the continental shelf. In Section 3.3, an approximation of the hydraulic control theory aims to explain how tides, stratification and bathymetry act on positioning of the salinity front. These are also fundamental on defining the position of the maximum turbidity region. In Section 4 we discuss the role of tides in fine sediment patch distribitions. Conversely, patches of fine sediments reduces the bottom drag coeficent and promotes tidal sea level and current amplification.
Another consequence of sediment distribution in marine environments may lead to generation of residual vorticity, which arises from non-linear interactions of currents on vicinity of different sediment patches regions. Also in Section 4 we discuss the role of anisotropy of sediment distribution on generating residual circulation in the ASD.

2. Characteristics of the Amazon Shelf Region

The Amazon Subaqueous Delta is part of the Amazon Continental Shelf (North Brazil), which still is a relatively well preserved region and almost free of anthropogenic influences, although significant human influences in the Amazon Basin was already present long time ago in oscillations of the river discharge (Richey et al., 1989). The Amazon River discharge varies

seasonally and may be modulated by teleconnection anomalies, as that imposed by the El Niño-Southern Oscillation (ENSO) phenomenon. The mean annual discharge at the river mouth is about 2.0 10^5 m^3s^{-1}, which roughly represents 10% of overall freshwater input into the global ocean system.

The ARE does not fit into a classical definition of estuary due to its characteristics of broad extension and huge discharge (Miranda et al., 2002). Also, the estuarine mixing zone is not constrained by the estuary margins. The salinity front and the maximum turbidity region develop further ahead from the river mouth, which does not occur in a regular estuary.

As the AS is located right at the the equator, there is geostrophy degeneration on the momentum equations and equilibrium is achieved trought others terms. This promotes a very energetic environment where the barotropic tides are fundamental on circulation and mixing processes. Winds and waves are moderated in this region and do not have relative importance on the local dynamics, although it may be relevant on ressuspension and sediment transport during extreme events.

Former studies as (Beardsley et al., 1995; Fontes et al., 2008; Gabioux et al., 2005; Geyer et al., 1996), among others, have measured or modeled the tidal amplification due to supression of the bottom stress, imposed by fluid mud layers. The bathymetry and site locations in the AS are in Fig. 1.

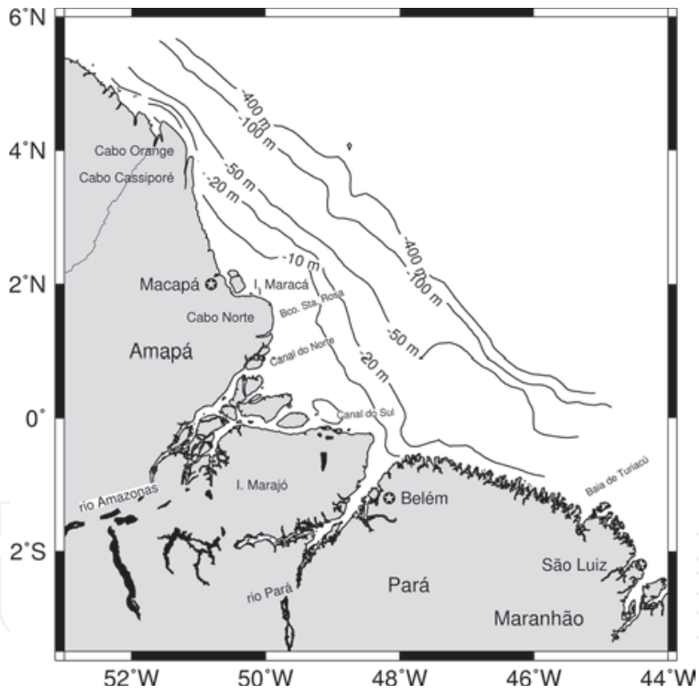

Fig. 1. Site locations in the Amazon Shelf and bathymetry representation.

3. Data & methods

We used the dataset and information provided from the former 1990's AMASSEDS Project, a multidisciplinary effort for compreension of sediment transport on the continental shelf near the Amazon River mouth (AMASSedS, 1990). Measurements of currents, salinity and temperature, tides and sediment concentration were available for proper modeling calibration and validation, mostly derived from the compilation in Alessi et al. (1992).

3.1 The ECOMSED numerical model

The Estuarine and Coastal Ocean Model and Sediment Trasport (ECOMSED) is an integrated suite of fortran routines for solving hydrodynamics and sediment transport in estuaries and coastal seas (Blumberg, 1996). The development of this suite has its origins with the Princeton Ocean Model (POM), a pioneer and consagrated model applied in ocean research (Blumberg & Mellor, 1980; 1983). The model is based on a three-dimensional set of equations that describes the geophysical fluid from the Naavier-Stokes formulation under the slallow water and Boussinesq approximations. The primitive equations solve the horizontal mode terms, including geostrophy and the baroclinic effect. The parameterization of Reynolds stress and flux terms account for the turbulent diffusion of salt, heat and momentum. The vertical mixing coefficients are obtained by solution of a second-order turbulence scheeme described in Mellor & Yamada (1982).

We applied a lattice with 81×181 horizontal grid cells and 17 vertical levels. The vertical $z-$coordinate fomulation is redefined in terms of σ-coordinates, in order to better represent the geometry of bottom and subsurface boundaries layers, in both shallow and deeper portions of the AS.

The sediment transport module (SED) employs the hydrodynamic results from the hydrodynamic core, in the same numerical grid. This SED module simulates the transport of suspended sediments for cohesive and non-cohesive sediment classes, as well as deposition, ressuspension and bed armoring. The same dynamic features from the hydrodynamic core are employed in the SED module: temperature, salinity, viscosity and turbulence diffusivity. For ordinary estuarine ocean models, density is primarly a function of temperature and salinity. As the ASD is also characterized for having substantial large nepheloid layers of high concentration of sediments, these fluid mud layer affects sea water density, amongst salinity and temperature Felix et al. (2006).

We included the contribution of cohesive sediment concentration in density calculation as in Wang (2002),

$$\rho = \rho_w + (1 - \frac{\rho_w}{\rho_s})C \tag{1}$$

where ρ_w is the clear water density, ρ_s is the cohesive sediment density and C is the suspended sediment concentration.

The suspended transport of fine sands is calculated using the van Rijn's method (van Rijn, 1993). The bed load transport is not considered in this module because most of the sediment transport in marine system is in suspension as the rate of moviment of coarse materials is limited by the transport capacity of the environmental flow Haan et al. (1994).

3.2 Effect of sediments on hydrodynamics

Wang (2002) studied the dynamics of nepheloid layer in an idealized estuary, considering the coulpling effect of seawater and resuspended sediment concentration. The author found a two layer sediment distribution structure formed as a lutocline is developed above a nepheloid layer. A vertical sediment concentration gradient is of maximum at the former, and this vertical structure is found in regions as the ASD.

Bottom shear stress and the dynamics of the bottom boundary layer (bbl) in shallow marine environments are highly influenced by winds and currents, as well as distribution of sediment classes and its nature. The presence of submersed hills and valleys, mud deposits and bottom roughness are also relevant on the bbl dynamics. Near the bottom, the bottom stress and the turbulent kinetic energy are due to the combined effect of wave and currents (Grant &

Madsen, 1986). The parameterization of the drag coefficient (C_d) depends on structure of the water-bed interface,

$$C_d = \frac{\kappa^2}{\ln^2(z/z_o)} \tag{2}$$

where κ is the von Kármán's constant; z is the height in the bbl and z_o is the roughness length scale. Adams & Weatherly (1981) defined a vertical profile in the bbl based on extended consideration of combined physical, biological and morphological effects,

$$u(z) = \frac{u_*}{\kappa}[\log(\frac{z}{z_{oc}}) + \beta \int_{z_{oc}}^{z} \frac{Ri_H}{z}\, dz] \tag{3}$$

where Ri_H is the Richardson's Number as defined by Heathershaw (1979),

$$Ri_H = \frac{w_s\, \kappa\, z\, g\, c}{\rho\, u_*^3}(1 - \rho/\rho_s) \tag{4}$$

and,

w_s: sediment settling velocity;
c : concentration of sediments;
ρ_s: density of sediments.

The bottom stress ($C_d = u_*^2/u^2$) can be obtained from Equation 3,

$$C_d \approx \kappa^2/[(1 + 4.7 < Ri_H >)\, log(\frac{z}{z_{\circ c}})]^2 \tag{5}$$

where $< Ri_H >$ represents the vertical integrated Richardson's Number.
We prescribed the drag coefficient in the bbl directly from sediment distribution, instead applying the original model formulation. From Dyer (1986) we were able to relate a wide range of sediment classes with bottom roughness, considering a low stratified fluid into the bbl. We set this bottom stress formulation by compilation of sediment distribution over the AS (Fig. 2) and definition of fluid mud distributions obtained during the AMASSEDS Project. The the C_d modeling parameterization considered the sediment class and fluid mud distributions over the AS. Fluid mud regions have lowest C_d values while mud- and sand-mixtures assume intermediate values.

3.3 Approximation of the hydraulic control theory

The hydraulic control theory (HTC) must define the mechanisms for maintenance and positioning of the salinity front in the ASD and, therefore, relate it with the maximum turbidity zone definition.
(Chao & Paluszkiewicz, 1991) applyed the HCT on channels as in presence of lateral or bottom constrictions with two vertical density layers. Besides some restrictions on the aplication of HCT in marine environments, we used the approach developed by Cudaback & Jay (1996) in the Columbia River (OR, EUA). Fontes et al. (2008) followed the same method on the inner Amazon Shelf, near the river mouth.
According to the HCT, the river discharge may be subject to changes on its dynamical state, where the dynamic condition state turns from super-critical to sub-critical when it passes trough an internal hydraulic jump. A control point between the river mouth and the coastal zone defines the bottom salinity front and the maximum turbidity zone.

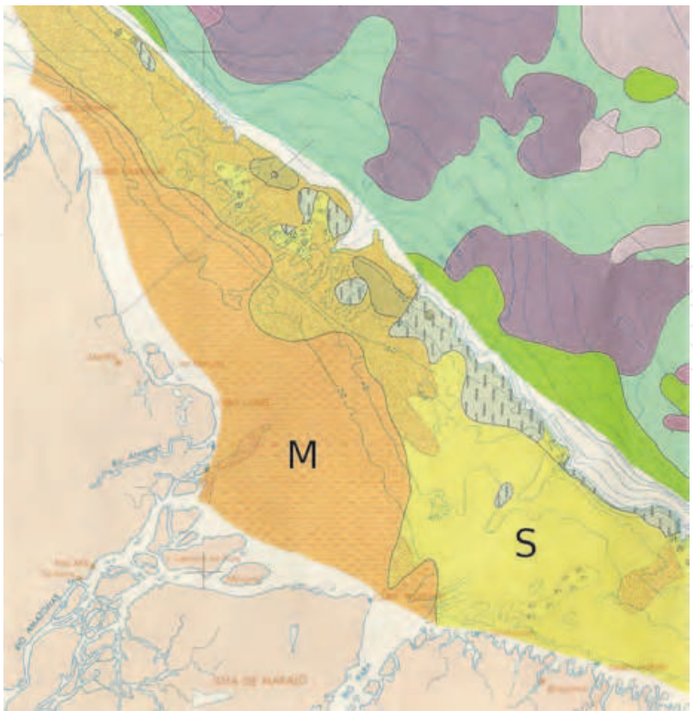

Fig. 2. Faciologic map of the Amazon Shelf from BRASIL (1979). Mud (M) and sand (S) sediment patches are annotated in the figure, representing regions of extreme C_d parametrization.

Armi & Farmer (1986) extended the application of HCT by defining an internal, or composite Froud number,

$$G^2 = F_1^2 + F_2^2 = \frac{u_1^2}{g'.h_1} + \frac{u_2^2}{g'.h_2} \tag{6}$$

where, $g' = g(\rho_1 - \rho_2)/\rho_1$ is the reduced gravity; ρ_i and h_i are density and layer thickness respectively [i=1(top),2(bottom)]; and F_i is the Froud number defined in each layer. This composite Froud number was calculated for an outflow cross shelf section at the Canal do Norte (North Channel).
The hydraulic control point occurs where the bottom slope is strongest, starting from -0.125 m km^{-1} and reaching up to -0.385 m km^{-1}. The region of maximum gradient in bathymetry occurs at 15 m deep, around 100 km from the coast. Figure 3 shows the line section along the ASD where the Froud number was evaluated.

3.4 Small scale vorticity generation mechanisms

Residual flow is an important effect in coastal oceanography and is commonly related to the subtidal flow, where tides and wind driving circulation are filtered out as well as other ambient influences. The residual influences are only due to rectification processes related to non-linear interactions from oscillatory flows. They are taken into account in the local circulation in order to affect advection. Regardless of that common assumption, it is convenient to redefine residual flow of a generic property a throughout a whole cycle of the

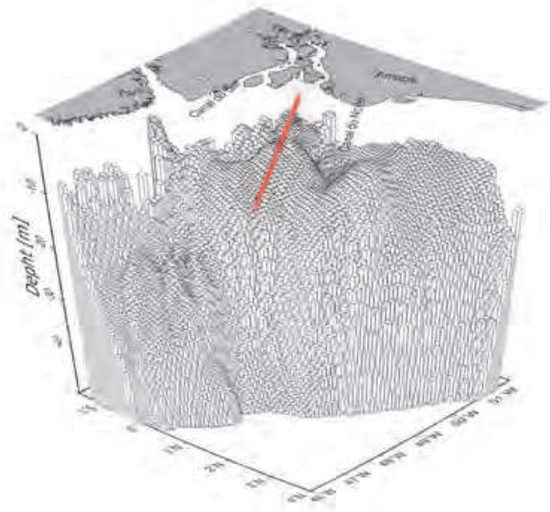

Fig. 3. ASD bathymetry representation and the section (red line) along with the Froud number was evaluated.

major tidal constituent M_2, as defined by Robinson (1983),

$$< a >= \frac{1}{T} \int_{t_0}^{t_0+T} a \, dt \tag{7}$$

where T is the period of the M_2 tidal component. In this case we are interested in the residual flow, so that depth integrated velocity at position x_0 is,

$$\vec{v} = \frac{1}{\bar{H} + \eta} \int_{-\bar{H}}^{\eta} \vec{v}_h \, dz \tag{8}$$

where $\bar{H}$ is the mean local depth. The residual term is named the Eulerian ($\vec{v}_E$), as properly justified, and is represented by integration over time,

$$\vec{v}_E = \frac{1}{T} \int_0^{t_0+T} \left(\frac{1}{\bar{H} + \eta} \int_{-\bar{H}}^{\eta} \vec{v}_h \, dz \right) dt \tag{9}$$

To retain the aspects of residual estimation we only considered the effects of tides (no winds, nor river discharge). Although tidal currents on the AS are energetic, their essentially oscillatory behavior does not result in significant net transport. The sediment load transport, for instance, is subject of long-term processes developed over the continental shelf, where residual flows can play a special feature on advection and consequently in the net transport. Residual flows can be generated by wind stress anisotropy over the shelf, by horizontal density gradients, horizontal gradients of sea surface due to remote processes or by non-linear tide interactions, when energy migrates from dominant frequencies to their harmonics and mean. It is known that tidal currents flowing over coastal areas subjected to irregular bathymetry produces residual flow due to non-linear interactions (Tee, 1994).

Anisotropy in the fields of properties like sediment distribution (bottom stress), Coriolis, bathymetry, velocity and dissipation are important on marine environments as the ASD. Those terms are defined from the vorticity Equation (Gross & Werner, 1994),

$$\frac{d\vec{\omega}}{dt} = -\frac{C_d|\vec{v}_H|}{H+\eta}\vec{\omega} + \frac{\vec{f}+\vec{\omega}}{H+\eta}\frac{d(H+\eta)}{dt} + \frac{C_D\vec{v}_H|\vec{v}_H|}{H+\eta} \times \left[\frac{\nabla_h|\vec{v}_H|}{|\vec{v}_H|} - \frac{\nabla_h(H+\eta)}{H+\eta} + \frac{\nabla_h C_D}{C_D}\right] \quad (10)$$

where $\omega = \frac{\partial v}{\partial x} - \frac{\partial u}{\partial y}$ is the vertical component of relative vorticity, $C_D = f(x,y)$ is the bottom stress horizontal distribution and $\vec{v}_H$ is the barotropic velocity. The η, H and f are sea surface displacement, depth and Coriolis' parameter, respectively.

4. Results

4.1 The Influence of tides on sediment dynamics

Using the same modeling dynamics described in Fontes et al. (2008), we considered the evaluation of cohesive sediments from the river discharge into the AS and ASD. The environmental dynamic conditions and charges of sediments represent climatological conditions of the AS, which are in Table 1,

Dynamical Mode	*Prognostic*
run time	600 h
River outflow discharge	2.0 $10^5 m^3 s^{-1}$
Salinity discharge	0.0
Temperature discharge	25.0°C
Cohesive sed. conc. in discharge	200 mg L^{-1}
Ambient initial salinity	35.0
Ambient initial temperature	25.0°C
Ambient coh. sed. conc.	5.00 mg L^{-1}
Spatially variable C_D	2.0 $10^{-4} \rightarrow$ 3.2 10^{-3}
Tidal components	semidiurnals Luni-solar and Solar M_2 and S_2
Winds	climatology (5.0 m s^{-1} - NE)

Table 1. Modeling conditions and parameterization for cohesive sediment transport in the ASD.

The evolution of cohesive sediment concentrations over the ASD is in Fig. 4 for both, bottom and surface distributions. When leaving the river mouth, they extend hundreds of kilometers Norhtwestward along the coast of Amapá. The higher concentrations at the bottom most layers ($>$ 10 mg L^{-1}) are better defined than the plume of sediments at the surface, where concentrations are at least one order of magnitude lesser than those near the bottom.
The formation and positioning of the sediment and salinity fronts (not shown) have similar dynamic aspects. Tides, bathymetry and the dynamical state represented by the Froud Number are capable of define them. The sediment dynamics differs by intrinsic phenomena as floculation and deposition, which are relevant in the formation of the nepheloid layers (concentrations above 10 gL^{-1}) as in Fig. 5.

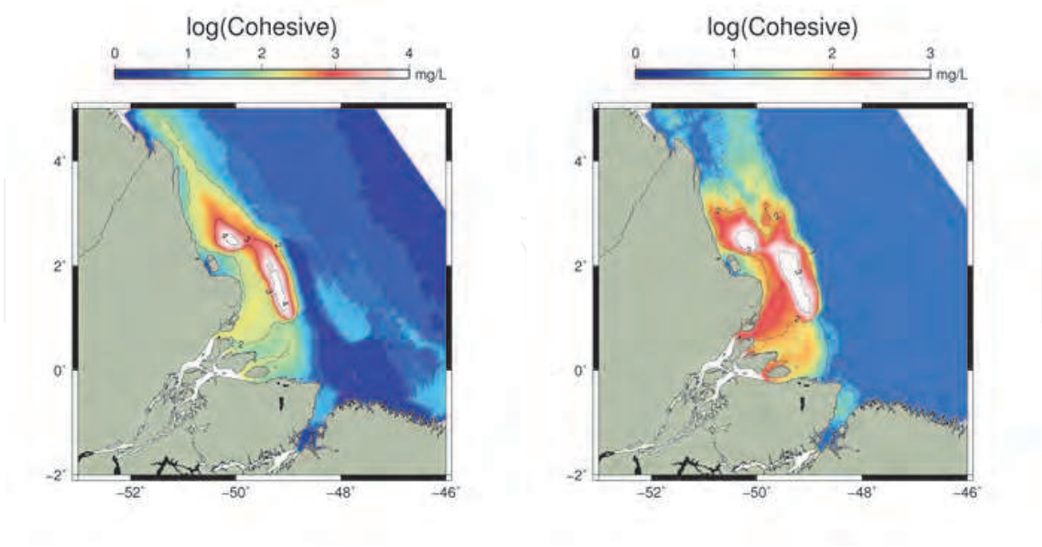

Fig. 4. Distribution of cohesive sediments in the bottom most (*left panel*) and near surface layer (*right panel*). Concentrations are in log_{10} scale and they differ in one order of magnitude.

4.2 Residual vorticity estimation

The tidal excursion along the ASD can promote residual vorticity when integrated between one tidal cicle, as previously described. For the ASD application we found the roughness gradient term the most important amongst the terms in Equation 10, regarding residual flux generation,

$$\frac{C_D \vec{v}_H |\vec{v}_H|}{H+\eta} \times \frac{\nabla_h C_D}{C_D}$$

The vorticity terms evaluated in the ASD are in Fig. 6, where the most relevant derives from integration and not from graphical correlation.

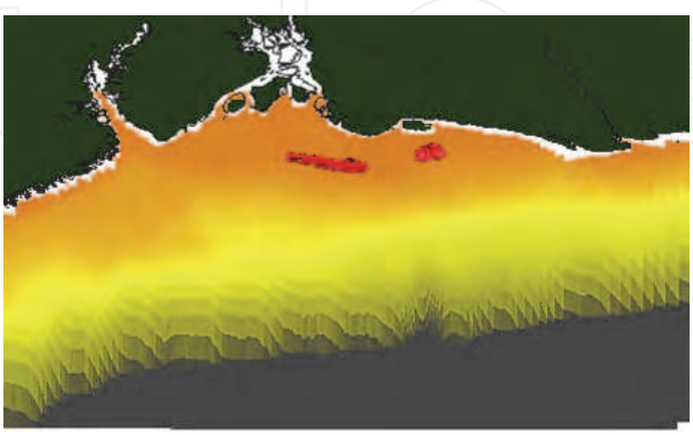

Fig. 5. Nepheloid layers located off Cabo Norte and Maraca Island. The red isosurface defines a 10 g L^{-1} concentration value for cohesive sediments.

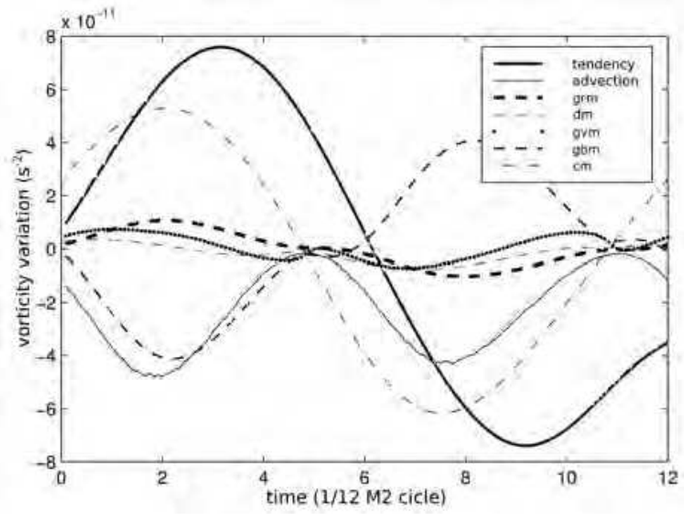

Fig. 6. Vorticity evaluated through 1 cycle of M_2 component, near Maracá Island (frontier of fluid mud region). The results are obtained according to Equation 10.

Estimation of residual flux was investigated through analysis of vorticity described on Section 3.4. For this residual flow estimation we choose a point located at the edge of the fluid mud frontier, nearby Maracá Island (Fig. 7). In coastal regions of the AS, the tidal ellipses are degenerated and highly polarized so they can be approximated by its rectilinear form,

$$\vec{\vec{q}} = \mathcal{V}\, cos\, \sigma t\, \vec{s} \tag{11}$$

according to a natural system of coordinates $(\vec{s}, \vec{n})$, where $\vec{s}$ is tangent to the stream current and $\vec{n}$ is the normal, left-oriented from the displacement. In this way, the vorticity Equation 10 in its scalar form can be expressed by:

$$\begin{aligned} \frac{\partial \omega}{\partial t} + \mathcal{V}\, cos\, \sigma t \frac{\partial \omega}{\partial s} &= A(s)\, cos\, \sigma t + \\ +[B(s) + B'(s)]\, cos\, \sigma t\, cos\, |\sigma t| - C(s)\, |cos\, \sigma t| \omega \end{aligned} \tag{12}$$

which is the Eulerian form as defined in Robinson (1983) and simplified by removing the lower order terms and making some other assumptions. σ is the M_2 tidal frequency, $\mathcal{V}$ is the tidal current amplitude in $\vec{s}$ direction,

$$A(s) = \frac{f\mathcal{V}}{H} \frac{\partial H}{\partial s}$$

$$B(s) = C_D\, \mathcal{V}\, \frac{\partial}{\partial n} (\mathcal{V}/H)$$

$$B'(s) = \frac{\mathcal{V}|\mathcal{V}|}{H} \frac{\partial C_D}{\partial n}$$

$$C(s) = \frac{C_D\, \mathcal{V}}{H}$$

are the terms of vorticity generation due to specific interactions: Coriolis mechanism **CM**; bathymetry and velocity gradients mechanism **GM**; roughness gradient mechanism **RM** and dissipative mechanism **DM**.The last term was held constant over the domain. A

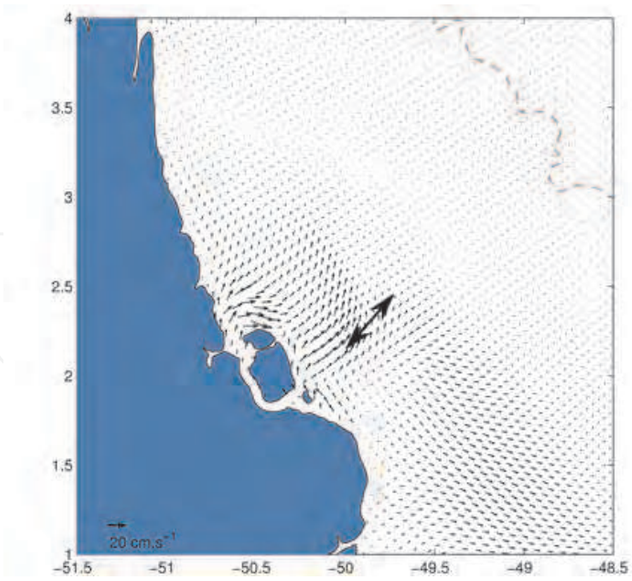

Fig. 7. Magnitude of the residual currents evaluated through one cycle of the M_2 tidal component, near Maracá Island. Higher values match transitional region of fluid-mud/bulk sediments.

detailed discussion considering different approaches for solving this problem can be found in Robinson (1983). At this point it is necessary to define a spatial scale related to residual vorticity,

$$E_M = [\frac{2}{T}\int_0^{T/2} \mathcal{V}\, sin\,(\sigma t)\, dt]\frac{T}{2} = \frac{\mathcal{V}}{\pi}\, T \tag{13}$$

Miranda et al. (2002) called this the "tidal excursion"; $T \approx 12.42$ h is the period of M_2. Estimation of the residual vorticity at the chosen point was made by computing the contributions of individual mechanisms listed above. Results were obtained by the model, considering that point and its neighborhood,

$$\begin{aligned}
\mathcal{V}(22,96) &= 1.5\, ms^{-1} \\
C_D(22,96) &= 3.27 \times 10^{-4} \\
H(22,96) &= 6.39\, m \\
\sigma_{M_2} &= 2.8 \times 10^{-4}\, s^{-1} \\
\partial n &\approx 8.15 \times 10^3 \\
\mathcal{V}(21,95) &= 1.3\, ms^{-1} \\
C_D(21,95) &= 2.0 \times 10^{-4} \\
H(21,95) &= 5.30\, m
\end{aligned}$$

The total residual vorticity computed at the point was $\omega_{res} = 2.11 \times 10^{-5}\, s^{-1}$. An estimation of residual velocity was obtained by applying the circulation theorem. Let the vorticity be

distributed over an area scaled by the tidal excursion, E_M. In this way, by applying Equation 13 it comes,

$$E_M = \frac{1.5}{\pi} 12.42(3600) = 2.1 \times 10^4 \ m$$

$$\mathcal{V}_{res} = \frac{\omega \pi (E_M/2)^2}{\pi E_M} \approx 0.1126 \ ms^{-1}$$

close to the value obtained by the model at that considered point, $\mathcal{V}'_{res} = 0.1193$.

5. Discussion and conclusions

Tides and the river discharge are the most energetic features on the inner Amazon Shelf dynamic system and promote, thought the hydraulic control theory, a reasonable explanation for positioning the salinity front and the maximum turbidity zone. Tides act as a stirring mechanism for the front generation and a control point located at 15 m depth, at the threshold, denotes where a hydraulic jump occurs.

We find the density field strongly affected by concentration of cohesive sediments, so this defines the formation of nepheloid layers in the ASD. The model reproduced the shape and position of fluid mud patches nearby Cabo Norte and MaracÃą Island, where concentrations were higher than 10 g L^{-1}.

Ocean color satellite imagery allows the retrieval of products such as particulate inorganic carbon (D. Clark personal communication, 2003). Fig. 8 illustrates an estimative of "climatological" sediment dispersion evaluated for the period of July 2002 through December 2007, with concentration value 2.0 10^{-2} mol m^{-3} denoting the higher values. Although the compilation of sattelite data has low resolution near the coast, it suffices to contour the influence of sediments in the ASD. Concentration values of the 4.0 10^{-2} mol m^{-3} isosurface defines a front that roughly matches the 100 mg L^{-1} isoline for cohesive sediment in the ASD (Fig. 4).

Although the large inertial flow imposed by the Amazon River accounts for most of the advection throughout the estuary, residual flow can locally contribute with long-term advective processes. This is mostly due to a rectification process that results from net transport integration throughout a semidiurnal tidal cycle. The tidally driven residual flow can contribute with advective processes such as sediment transport and pollutant advection and biological ones, as organic and larvae dispersion. As the Amazon River Estuary does not fit in the classical definition of the estuary, the high load sediment concentration flow occur in the ASD favoring the formation of mud deposits that extend for kilometers. Modeling the transport of cohesive sediments in marine environments, as the AS, requires parameterization of substantial oceanographic, meteorologic and sedimentological data. Others, like bathymetry and hydrology are equally fundamental. Also, parameterization of natural environments like estuaries and coastal seas is a hard task, most of the time, once those environments have distinct behavior from the test fluid in laboratories.

A broad scale of temporal and spatial phenomena (from turbulence to tides and mesoscale variations) and the unpredictable occurrence of extreme events as storms and oceanic rings from current systems. Models are not always capable to deal with phenomena like these. Nevertheless, they are usable since the problem definition and efforts on its implementation are focused on a narrower set of physical phenomena. Under the hydraulic control theory, the estuarine dynamics and the nature of sediments in the AS we were able to understand how physical aspects can act in the deposition and transport related phenomena.

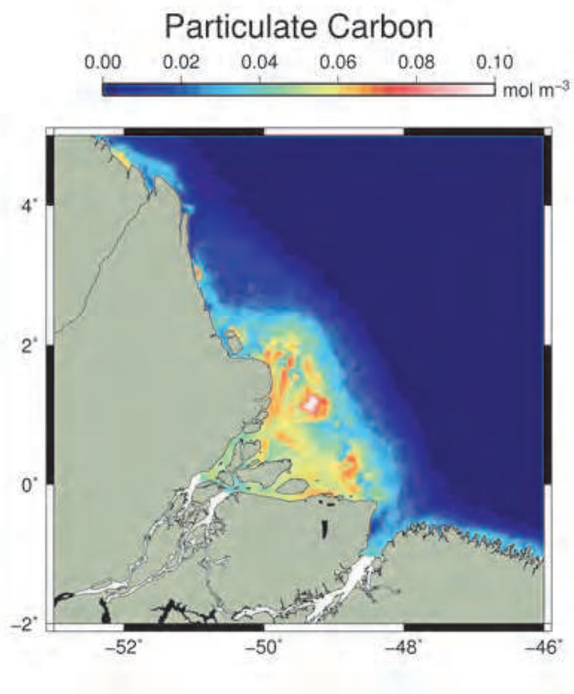

Fig. 8. Particulate inorganic carbon derived from sattelite imagery for the period of July 2002 through Dec. 2007 (D. Clark personal communication, 2003).

6. References

Adams, C. E. & Weatherly, G. L. (1981). Some effects of suspended sediment stratification on an oceanic bottom boundary layer, *J. geophys. Res.* (86): 4161–4172.

Alessi, C., Lentz, S. J., Beardsley, R. C., Castro, B. M. & Geyer, W. R. (1992). A multidisciplinary amazon shelf sediment study (amasseds): Physical oceanography moored array component, *Technical Report WHOI-92-36*, Woods Hole Oceanography Institution.

AMASSedS (1990). A multi-disciplinary amazon shelf sediment study (amasseds). Eos, Trans. AGU, 71, 1771.

Armi, L. & Farmer, D. M. (1986). Maximal two-layer exchange through a contraction with barotropic net flow, *J. Fluid Mech.* 164: 27–51.

Beardsley, R. C., Candela, J., Limeburner, R., Geyer, W. R., Lentz, S. J., Castro, B. M., Cacchione, D. & Carneiro, N. (1995). The m2 tide in the amazon shelf, *J. geophys. Res.* 100(C2): 2283–2319.

Blumberg, A. F. (1996). An estuarine and coastal ocean version of pom, *Proceedings of the Princeton Ocean Model Users Meeting (POM96)*.

Blumberg, A. F. & Mellor, G. L. (1980). A coastal ocean numerical model, *in* J. Sundermann & K. P. Holz (eds), *Mathematical Modelling of Estuarine Physics, Proceedings of an International Symposium*, Spring-Verlag, Berlin.

Blumberg, A. F. & Mellor, G. L. (1983). Diagnostic and prognostic numerical circulation studies of the south atlantic bight, *J. geophys. Res.* (88): 4579–4592.

BRASIL (1979). Margem continental norte: Mapa faciológico dos sedimentos superficiais da plataforma e da sedimentação quaternária no oceano profundo, cartographic chart, scale=1:3.500.000. Projeto REMAC - Reconhecimento Global da Margem Continental Brasileira.

Chao, S.-Y. & Paluszkiewicz, T. (1991). The hydraulics of density currents over estuarine sills, *J. Geophys. Res.* 96(C4): 7065–7076.

Cudaback, C. N. & Jay, D. A. (1996). Formation of columbia river plume: Hydraulic control in action?, *in* D. G. Aubrey & C. T. Friedrichs (eds), *Buoyance Effects on Coastal and Estuarine Dynamics*, Vol. 53 of *Coastal and Estuarine Studies*, American Geophysical Union, Washington, DC, pp. 139–174.

Dyer, K. R. (1986). *Coastal and estuarine sediment dynamics*, John Wiley and Sons Ltd., Great Britain.

Felix, M., Peakall, J. & McCaffrey, W. D. (2006). Relative importance of processes that govern the generation of particulate hyperpycnal flows, *Journal of Sedimentary Research* 76: 382–387.

Fontes, R. F. C., Castro, B. M. & Beardsley, R. C. (2008). Numerical study of circulation on the inner amazon shelf, *Ocean Dynamics* .

Gabioux, M., Vinzon, S. B. & Paiva, A. M. (2005). Tidal propagation over fluid mud layers on the amazon shelf, *Continental Shelf Research* (25): 113–125.

Geyer, W. R., Beardsley, R. C., Lentz, S. J., Candela, J., Limeburner, R., Johns, W. E., Castro, B. M. & Soares, I. D. (1996). Physical oceanography of the amazon shelf, *Continent. Shelf Res.* 5/6(16): 575–616.

Grant, W. D. & Madsen, O. S. (1986). The continental-shelf bottom boundary layer, *Ann. Rev. Fluid Mech.* 18: 265–305.

Gross, T. F. & Werner, F. E. (1994). Residual circulations due to bottom roughness variability under tidal flows, *J. phys. Oceanogr.* 24: 1494–1502.

Haan, C. T., Barfield, B. J. & Hayes, J. C. (1994). *Design Hydrology and Sedimentology for Small Catchments*, Academic Press, Inc.

Heathershaw, A. D. (1979). The turbulent structure of the bottom boundary layer in a tidal current, *Geophys. J. Astron. Soc.* 58: 395–430.

Kineke, G. C., Sternberg, R. W., Trowbridge, J. H. & Geyer, W. R. (1996). Fluid-mud processes on the amazon continental shelf, *Continent. Shelf Res.* 16(5/6): 667–696.

Mellor, G. & Yamada, T. (1982). Development of a turbulence closure model for geophysical fluid problems, *Revs. Geophys. Space Phys.* (20): 851–875.

Miranda, L. B., Castro, B. M. & Kjefve, B. (2002). *Principios de Oceanografia Fisica de Estuarios*, Edusp.

Richey, J. E., Nobre, C. & Deser, C. (1989). Amazon river discharge and climate variability: 1903 to 1985, *Science, New Series* 246(4926): 101–103.

Robinson, I. (1983). *Tidally induced residual flows*, Elsevier Oceanography Series, 35, Elsevier, Whiteknights, England. Physical oceanography of coastal and shelf seas.

Tee, K. T. (1994). Dynamics of a two-dimensional topographic rectification process, *J. phys. Oceanogr.* 24.

van Rijn, L. C. (1993). *Principles of sediment transport in rivers, estuaries and coastal seas*, Aqua Publications, Amsterdam.

Wang, X. H. (2002). Tide-induced sediment resuspension and the bottom boundary layer in an idealized estuary with a muddy bed, *Journal of Physical Oceanography* 32: 3113–3131.

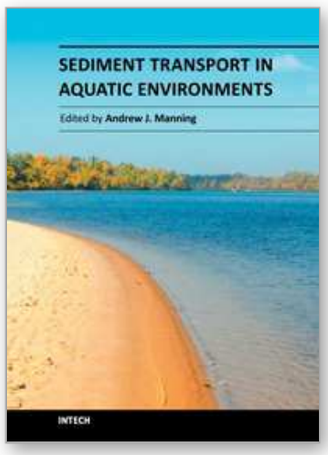

Sediment Transport in Aquatic Environments

Edited by Dr. Andrew Manning

ISBN 978-953-307-586-0

Hard cover, 332 pages

Publisher InTech

Published online 30, September, 2011

Published in print edition September, 2011

Sediment Transport in Aquatic Environments is a book which covers a wide range of topics. The effective management of many aquatic environments, requires a detailed understanding of sediment dynamics. This has both environmental and economic implications, especially where there is any anthropogenic involvement. Numerical models are often the tool used for predicting the transport and fate of sediment movement in these situations, as they can estimate the various spatial and temporal fluxes. However, the physical sedimentary processes can vary quite considerably depending upon whether the local sediments are fully cohesive, non-cohesive, or a mixture of both types. For this reason for more than half a century, scientists, engineers, hydrologists and mathematicians have all been continuing to conduct research into the many aspects which influence sediment transport. These issues range from processes such as erosion and deposition to how sediment process observations can be applied in sediment transport modeling frameworks. This book reports the findings from recent research in applied sediment transport which has been conducted in a wide range of aquatic environments. The research was carried out by researchers who specialize in the transport of sediments and related issues. I highly recommend this textbook to both scientists and engineers who deal with sediment transport issues.

InTech Europe

University Campus STeP Ri
Slavka Krautzeka 83/A
51000 Rijeka, Croatia
Phone: +385 (51) 770 447
Fax: +385 (51) 686 166

InTech China

Unit 405, Office Block, Hotel Equatorial Shanghai
No.65, Yan An Road (West), Shanghai, 200040, China
中国上海市延安西路65号上海国际贵都大饭店办公楼405单元
Phone: +86-21-62489820
Fax: +86-21-62489821

IntechOpen

IntechOpen